



Observation of a χ'_{c2} candidate in $\gamma\gamma \rightarrow D\bar{D}$ production at Belle

S. Uehara,⁸ K. Abe,⁸ K. Abe,³⁹ I. Adachi,⁸ H. Aihara,⁴¹ K. Arinstein,¹ Y. Asano,⁴⁵ V. Aulchenko,¹ T. Aushev,¹³
A. M. Bakich,³⁶ V. Balagura,¹³ E. Barberio,²⁰ I. Bedny,¹ K. Belous,¹¹ U. Bitenc,¹⁴ I. Bizjak,¹⁴ S. Blyth,²³
A. Bondar,¹ A. Bozek,²⁵ M. Bračko,^{8,19,14} T. E. Browder,⁷ M.-C. Chang,⁴⁰ A. Chen,²³ W. T. Chen,²³
B. G. Cheon,³ R. Chistov,¹³ S.-K. Choi,⁶ Y. Choi,³⁵ Y. K. Choi,³⁵ A. Chuvikov,³¹ J. Dalseno,²⁰ M. Danilov,¹³
M. Dash,⁴⁶ J. Dragic,⁸ S. Eidelman,¹ D. Epifanov,¹ S. Fratina,¹⁴ N. Gabyshev,¹ A. Garmash,³¹ T. Gershon,⁸
G. Gokhroo,³⁷ A. Gorišek,¹⁴ H. C. Ha,¹⁶ K. Hayasaka,²¹ H. Hayashii,²² M. Hazumi,⁸ L. Hinz,¹⁸ Y. Hoshi,³⁹
S. Hou,²³ T. Iijima,²¹ K. Inami,²¹ A. Ishikawa,⁸ R. Itoh,⁸ M. Iwasaki,⁴¹ Y. Iwasaki,⁸ N. Katayama,⁸ H. Kawai,²
T. Kawasaki,²⁶ H. Kichimi,⁸ H. J. Kim,¹⁷ S. M. Kim,³⁵ S. Korpar,^{19,14} P. Krokovny,¹ R. Kulasiri,⁴ C. C. Kuo,²³
A. Kuzmin,¹ Y.-J. Kwon,⁴⁷ J. S. Lange,⁵ G. Leder,¹² S. E. Lee,³³ T. Lesiak,²⁵ J. Li,³² S.-W. Lin,²⁴ D. Liventsev,¹³
F. Mandl,¹² T. Matsumoto,⁴³ A. Matyja,²⁵ W. Mitaroff,¹² K. Miyabayashi,²² H. Miyata,²⁶ Y. Miyazaki,²¹
R. Mizuk,¹³ T. Nagamine,⁴⁰ Y. Nagasaka,⁹ E. Nakano,²⁸ M. Nakao,⁸ H. Nakazawa,⁸ S. Nishida,⁸ O. Nitoh,⁴⁴
S. Ogawa,³⁸ T. Ohshima,²¹ T. Okabe,²¹ S. Okuno,¹⁵ S. L. Olsen,⁷ P. Pakhlov,¹³ C. W. Park,³⁵ H. Park,¹⁷
R. Pestotnik,¹⁴ L. E. Piilonen,⁴⁶ A. Poluektov,¹ Y. Sakai,⁸ N. Sato,²¹ N. Satoyama,³⁴ T. Schietinger,¹⁸
O. Schneider,¹⁸ K. Senyo,²¹ M. E. Sevier,²⁰ M. Shapkin,¹¹ H. Shibuya,³⁸ B. Shwartz,¹ V. Sidorov,¹ J. B. Singh,²⁹
A. Sokolov,¹¹ A. Somov,⁴ N. Soni,²⁹ R. Stamen,⁸ S. Stanič,²⁷ M. Starič,¹⁴ T. Sumiyoshi,⁴³ F. Takasaki,⁸
K. Tamai,⁸ N. Tamura,²⁶ M. Tanaka,⁸ G. N. Taylor,²⁰ X. C. Tian,³⁰ K. Trabelsi,⁷ T. Tsukamoto,⁸ T. Uglov,¹³
K. Ueno,²⁴ S. Uno,⁸ P. Urquijo,²⁰ Y. Usov,¹ G. Varner,⁷ Y. Watanabe,⁴² E. Won,¹⁶ Q. L. Xie,¹⁰ B. D. Yabsley,⁴⁶
A. Yamaguchi,⁴⁰ M. Yamauchi,⁸ J. Ying,³⁰ C. C. Zhang,¹⁰ J. Zhang,⁸ L. M. Zhang,³² Z. P. Zhang,³² and V. Zhilich¹

(The Belle Collaboration)

¹*Budker Institute of Nuclear Physics, Novosibirsk*

²*Chiba University, Chiba*

³*Chonnam National University, Kwangju*

⁴*University of Cincinnati, Cincinnati, Ohio 45221*

⁵*University of Frankfurt, Frankfurt*

⁶*Gyeongsang National University, Chinju*

⁷*University of Hawaii, Honolulu, Hawaii 96822*

⁸*High Energy Accelerator Research Organization (KEK), Tsukuba*

⁹*Hiroshima Institute of Technology, Hiroshima*

¹⁰*Institute of High Energy Physics, Chinese Academy of Sciences, Beijing*

¹¹*Institute of High Energy Physics, Protvino*

¹²*Institute of High Energy Physics, Vienna*

¹³*Institute for Theoretical and Experimental Physics, Moscow*

¹⁴*J. Stefan Institute, Ljubljana*

¹⁵*Kanagawa University, Yokohama*

¹⁶*Korea University, Seoul*

¹⁷*Kyungpook National University, Taegu*

¹⁸*Swiss Federal Institute of Technology of Lausanne, EPFL, Lausanne*

¹⁹*University of Maribor, Maribor*

²⁰*University of Melbourne, Victoria*

²¹*Nagoya University, Nagoya*

²²*Nara Women's University, Nara*

²³*National Central University, Chung-li*

²⁴*Department of Physics, National Taiwan University, Taipei*

²⁵*H. Niewodniczanski Institute of Nuclear Physics, Krakow*

²⁶*Niigata University, Niigata*

²⁷*Nova Gorica Polytechnic, Nova Gorica*

²⁸*Osaka City University, Osaka*

²⁹*Panjab University, Chandigarh*

- ³⁰*Peking University, Beijing*
³¹*Princeton University, Princeton, New Jersey 08544*
³²*University of Science and Technology of China, Hefei*
³³*Seoul National University, Seoul*
³⁴*Shinshu University, Nagano*
³⁵*Sungkyunkwan University, Suwon*
³⁶*University of Sydney, Sydney NSW*
³⁷*Tata Institute of Fundamental Research, Bombay*
³⁸*Toho University, Funabashi*
³⁹*Tohoku Gakuin University, Tagajo*
⁴⁰*Tohoku University, Sendai*
⁴¹*Department of Physics, University of Tokyo, Tokyo*
⁴²*Tokyo Institute of Technology, Tokyo*
⁴³*Tokyo Metropolitan University, Tokyo*
⁴⁴*Tokyo University of Agriculture and Technology, Tokyo*
⁴⁵*University of Tsukuba, Tsukuba*
⁴⁶*Virginia Polytechnic Institute and State University, Blacksburg, Virginia 24061*
⁴⁷*Yonsei University, Seoul*

We report on a search for new resonant states in the process $\gamma\gamma \rightarrow D\bar{D}$. A candidate C -even charmonium state is observed in the vicinity of $3.93 \text{ GeV}/c^2$. The production rate and the angular distribution in the $\gamma\gamma$ center-of-mass frame suggest that this state is the previously unobserved χ'_{c2} , the 2^3P_2 charmonium state.

PACS numbers: 13.66.Bc, 14.40.Gx

The masses and other properties of the ground and excited states of charmonium provide valuable input to QCD models that describe heavy quarkonium systems. To date, radial excitation states of charmonium are established only for the $^{2S+1}L_J = ^3S_1$ (ψ) and, recently, the 1S_0 (η_c) [1] states. Although the lowest 3P_J states (χ_{cJ}) are already well established, their radial excitations have not yet been observed.

The first radially excited χ_{cJ} states are predicted to have masses between 3.9 and $4.0 \text{ GeV}/c^2$ [2, 3], which is considerably above $D\bar{D}$ threshold. If the masses of these states lie between the $D\bar{D}$ and $D^*\bar{D}^*$ thresholds, the $\chi_{c0}(2P)$ (χ'_{c0}) and $\chi_{c2}(2P)$ (χ'_{c2}) are expected to decay primarily into $D\bar{D}$, although the χ'_{c2} could also decay to $D\bar{D}^*$ if it is energetically allowed. (The inclusion of charge-conjugate reactions is implied throughout this paper.) Recently, two new charmonium-like states in this mass region, the $X(3940)$ [4] and $Y(3940)$ [5], were reported by Belle. Neither of these states has been observed to decay to $D\bar{D}$ [4].

In this paper we report on a search for the χ'_{cJ} ($J = 0$ or 2) states and other C -even charmonium states in the mass range of $3.73 - 4.3 \text{ GeV}/c^2$ produced via the process $\gamma\gamma \rightarrow D\bar{D}$.

The analysis uses data recorded in the Belle detector at the KEKB e^+e^- asymmetric-energy (3.5 on 8 GeV) collider [6]. The data sample corresponds to an integrated luminosity of 395 fb^{-1} , accumulated on the $\Upsilon(4S)$ resonance ($\sqrt{s} = 10.58 \text{ GeV}$) and 60 MeV below the resonance. We study the two-photon process $e^+e^- \rightarrow e^+e^-D\bar{D}$ in the “zero-tag” mode, where neither the final-state electron nor positron is detected, and the $D\bar{D}$ system has very small transverse momentum.

A comprehensive description of the Belle detector is given elsewhere [7]. Charged tracks are reconstructed in a central drift chamber (CDC) located in a uniform 1.5 T solenoidal magnetic field. The z axis of the detector and the solenoid are along the positron beam, with the positrons moving in the $-z$ direction. Track trajectory coordinates near the collision point are measured by a silicon vertex detector (SVD). Photon detection and energy measurements are provided by a CsI(Tl) electromagnetic calorimeter (ECL). Silica-aerogel Cherenkov counters (ACC) provide separation between kaons and pions for momenta above $1.2 \text{ GeV}/c$. The time-of-flight counter (TOF) system consists of a barrel of 128 plastic scintillation counters, and is effective for K/π separation for tracks with momenta below $1.2 \text{ GeV}/c$. Low energy kaons are also identified by specific ionization (dE/dx) measurements in the CDC.

Kaon candidates are separated from pions based on normalized kaon and pion likelihood functions obtained from the particle identification system (L_K and L_π , respectively) with a criterion, $L_K/(L_K + L_\pi) > 0.8$, which gives a typical identification efficiency of 90% with a probability of 3% for a pion to be misidentified as a kaon. All tracks that are not identified as kaons are treated as pions.

Signal candidates are triggered by a variety of track-triggers that require two or more CDC tracks with associated TOF hits, ECL clusters or a minimum sum of energy in the ECL. For the four and six charged track topologies used in this analysis, the trigger conditions are complementary to each other and, in combination, provide a high trigger efficiency, $(96 \pm 3)\%$.

We search for exclusive $D\bar{D}$ production in the following

four combinations of decays:

$$\gamma\gamma \rightarrow D^0\bar{D}^0, D^0 \rightarrow K^-\pi^+, \bar{D}^0 \rightarrow K^+\pi^- \quad (\text{N4}),$$

$$\gamma\gamma \rightarrow D^0\bar{D}^0, D^0 \rightarrow K^-\pi^+, \bar{D}^0 \rightarrow K^+\pi^-\pi^0 \quad (\text{N5}),$$

$$\gamma\gamma \rightarrow D^0\bar{D}^0, D^0 \rightarrow K^-\pi^+, \bar{D}^0 \rightarrow K^+\pi^-\pi^+\pi^- \quad (\text{N6}),$$

$$\gamma\gamma \rightarrow D^+D^-, D^+ \rightarrow K^-\pi^+\pi^+, D^- \rightarrow K^+\pi^-\pi^- \quad (\text{C6}).$$

The symbols in parentheses are used to designate each of the final states. For the four-prong processes (N4 and N5) the selection criteria are: four charged tracks, each one with (L) a transverse momentum to the z axis in the laboratory frame of $p_t > 0.1$ GeV/ c ; two or more tracks must have (S) $p_t > 0.4$ GeV/ c and $17^\circ < \theta < 150^\circ$, where θ is the laboratory frame polar angle; no photon clusters with an energy greater than 400 MeV; the charged track system consists of a $K^+K^-\pi^+\pi^-$ combination; the $K^\pm\pi^\mp$ combination with the larger invariant mass should lie within ± 15 MeV/ c^2 of the nominal D^0 mass. For the N4 process, we require that the $K^\pm\pi^\mp$ combination with the smaller invariant mass be within $^{+15}_{-20}$ MeV/ c^2 of the nominal D^0 mass. For the N5 process, we require that the remaining $K\pi$ combination, when combined with a π^0 candidate, has an invariant mass in the range 1.83 GeV/ $c^2 < M(K^+\pi^-\pi^0) < 1.89$ GeV/ c^2 . Candidate π^0 's are formed from pairs of photons with energies greater than 20 MeV, which fit to the $\pi^0 \rightarrow \gamma\gamma$ hypothesis with $\chi^2 < 4$. If there are multiple π^0 candidates, we select the one that results in $M(K^+\pi^-\pi^0)$ closest to the nominal D^0 mass.

For the six-prong processes (N6 and C6), we require exactly six tracks with particle assignments $K^+K^-\pi^+\pi^-\pi^+\pi^-$, where all six pass the looser track criteria, indicated by (L) above. In addition, either two to four tracks must pass the more stringent track criteria (S) or at least one track has $p_t > 0.5$ GeV/ c and the sum of ECL cluster energies is less than $0.18\sqrt{s}$, where the cluster energies are measured in the e^+e^- center-of-mass (c.m.) system. For the N6 process, one combination is required to have $|\Delta M|_1 = |M(K^+\pi^-) - m_{D^0}| < 15$ MeV/ c^2 while the remaining tracks have $|\Delta M|_2 = |M(K^-\pi^+\pi^-\pi^+) - m_{D^0}| < 30$ MeV/ c^2 . When there are multiple combinations, we choose the one with the smallest $|\Delta M|_1 + |\Delta M|_2$. For the C6 process, we require $|M(K^\mp\pi^\pm\pi^\pm) - m_{D^\pm}| < 30$ MeV/ c^2 for each of the charge combinations, where m_{D^\pm} is the nominal D^\pm mass.

For all processes, we require that there be no extra π^0 candidates with transverse momenta larger than 100 MeV/ c . We also apply the following kinematical requirement to the $D\bar{D}$ candidate system: $P_z(D\bar{D}) > (M(D\bar{D})^2 - 49 \text{ GeV}^2/c^4)/(14 \text{ GeV}/c^3) + 0.6$ GeV/ c , where $P_z(D\bar{D})$ and $M(D\bar{D})$ are the momentum component in the z direction in the laboratory frame and the invariant mass, respectively. This condition removes events from initial-state radiation (ISR) processes, such as $e^+e^- \rightarrow D^{(*)}\bar{D}^{(*)}\gamma$, in which the photon is emit-

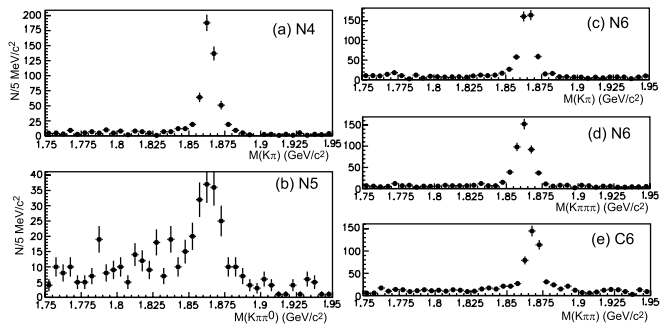


FIG. 1: Invariant mass distributions of (a) $K^\mp\pi^\pm$ in N4 candidate events, (b) $K^\pm\pi^\mp\pi^0$ in N5 candidate events, (c) $K^\mp\pi^\pm$ in N6 candidate events, (d) $K^\pm\pi^\mp\pi^\pm\pi^\mp$ in N6 candidate events, and (e) $K^\pm\pi^\mp\pi^\mp$ in C6 candidate events. An accompanying D meson candidate is required in each event sample.

ted in the forward direction with respect to the incident electron. We compute $M(D\bar{D})$ using the measured 3-momenta of each D candidate (P_D) and energy determined from $E_D = \sqrt{P_D^2 + m_D^2}$, where m_D is the nominal mass of the neutral or charged D .

The invariant mass distributions for D meson candidates reconstructed with the above requirements are shown in Fig. 1.

We calculate $P_t(D\bar{D})$, the total transverse momentum in the e^+e^- c.m. frame with respect to the incident e^+e^- axis that approximates the direction of the two-photon collision axis. We apply the requirement $P_t(D\bar{D}) < 0.05$ GeV/ c to enhance exclusive two-photon $\gamma\gamma \rightarrow D\bar{D}$ production. In the invariant mass region $M(D\bar{D}) < 4.3$ GeV/ c^2 , we find 86 N4-process events, 60 N5-process events, 168 N6-process events and 128 C6-process events.

In Figs. 2(a) and 2(b) we show the $M(D\bar{D})$ distributions separately for $D^0\bar{D}^0$ (sum of N4, N5 and N6) and D^+D^- . The invariant-mass distribution for the combined $D^0\bar{D}^0$ and D^+D^- channels is shown in Fig. 2(c). There, two event concentrations are evident: one near 3.80 GeV/ c^2 rather close to the threshold of $D\bar{D}$ and another near 3.93 GeV/ c^2 . Each distribution of the four decay combination modes shows an enhancement near the latter invariant mass. We apply an unbinned maximum likelihood fit to the combined data in the region $3.80 \text{ GeV}/c^2 < M(D\bar{D}) < 4.20 \text{ GeV}/c^2$ using a relativistic Breit-Wigner signal function for the resonant peak near 3.93 GeV/ c^2 plus a background of the form $M(D\bar{D})^{-\alpha}$, where α is a free parameter. The invariant mass dependence of the efficiency (decreasing by 10% for an increase of the invariant mass from 3.80 to 4.20 GeV/ c^2) and the two-photon luminosity function are taken into account in the resonance function. These are computed using the TREPS Monte-Carlo(MC) program [8] for $e^+e^- \rightarrow e^+e^-D\bar{D}$ production together with

JETSET7.3 decay routines [9] for the D meson decays (using PDG2004 [10] values for the decay branching fractions). We find from the MC study that the product of the efficiency and branching fractions of the two D decay modes in the D^+D^- channel is about 50% of that in the $D^0\bar{D}^0$ channel.

The results of the fit for the resonance mass, width and total yield of the resonance are $M = 3929 \pm 5(stat)$ MeV/ c^2 , $\Gamma = 29 \pm 10(stat)$ MeV and $64 \pm 18(stat)$ events, respectively. The mass resolution, which is estimated by MC to be 3 MeV/ c^2 is taken into account in the fit. The statistical significance of the peak is 5.3σ , which is derived from $\sqrt{2\ln(L_{\max}/L_0)}$, where L_{\max} and L_0 are the logarithmic-likelihoods for fits with and without a resonance peak component, shown in Fig. 2(c) as solid and dashed curves, respectively.

Systematic errors for the parameters M and Γ are 2 MeV/ c^2 and 2 MeV, respectively. The former is partially due to the uncertainties on the D meson masses (1 MeV/ c^2 for the resonance mass). We also consider the effect of choosing different Breit-Wigner functional forms for spin 0 and 2 resonances and wave functions in this error.

The $P_t(D\bar{D})$ distribution in the peak region, $3.91 \text{ GeV}/c^2 < M(D\bar{D}) < 3.95 \text{ GeV}/c^2$, is shown in Fig. 3. Here the P_t requirement has been relaxed. The experimental data are fitted by a shape that is expected for exclusive two-photon $D\bar{D}$ production plus a linear background. We expect non-charm and non-exclusive backgrounds to be nearly linear in $P_t(D\bar{D})$. The fit uses a binned-maximum likelihood method with the normalizations of the two components treated as free parameters. The linear-background component, 1.8 ± 0.6 events for $P_t(D\bar{D}) < 0.05 \text{ GeV}/c^2$, and the goodness of fit, $\chi^2/d.o.f. = 14.2/18$, indicate that the events in the peak region originate primarily from exclusive two-photon events.

The $P_t(D\bar{D})$ distribution produced by $D\bar{D}^*$ and $D^*\bar{D}^*$ events is expected to be distorted by the transverse momentum of the undetected slow pion(s), which peaks around 0.05 GeV/ c (dashed histogram in Fig. 3). Such a distortion is not seen in the observed P_t distribution.

We investigate possible backgrounds from non- $D\bar{D}$ sources using D -sideband events. The histogram in Fig. 2(c) shows the invariant mass distribution for events where the D -meson is replaced by a hadron system from a D -signal mass sideband regions above and below the signal region with the same width as the signal mass region. Here we use two types of sideband events: one where one D -meson candidate is in the signal mass region, and another where both entries are from the sidebands. Since there is no significant event excess in the former type over the latter, we conclude that the sideband events are dominated by non-charm backgrounds. We combine them and appropriately scale in order to compare to the $D\bar{D}$ signal yield. We conclude that the candidate events are domi-

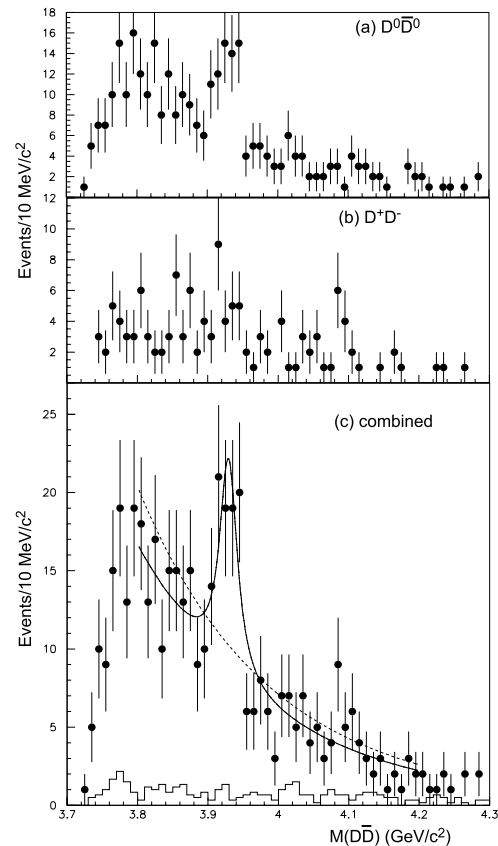


FIG. 2: Invariant mass distributions for the (a) $D^0\bar{D}^0$ channels and (b) the D^+D^- mode. (c) The combined $M(D\bar{D})$ distribution. The curves show the fits with (solid) and without (dashed) a resonance component. The histogram shows the distribution of the events from the D -mass sidebands (see the text).

nated by $D\bar{D}$ (inclusive or exclusive) events in the entire mass region.

Figures 4(a) and (b) show the $M(D\bar{D})$ distributions for events with $|\cos\theta^*| < 0.5$ and $|\cos\theta^*| > 0.5$, respectively, where θ^* is the angle of a D meson relative to the beam axis in the $\gamma\gamma$ c.m. frame. It is apparent that the events in the 3.93 GeV/c^2 peak tend to concentrate at small $|\cos\theta^*|$ values. The points with error bars in Fig. 4(c) show the event yields in the 3.91 GeV/c^2 to 3.95 GeV/c^2 region versus $|\cos\theta^*|$. Background, estimated from events in the $M(D\bar{D})$ sideband, is indicated by the histogram. The solid curve in Fig. 4(c) shows the expectation using $\sin^4\theta^*$ to represent the signal from a spin-2 meson produced with helicity-2 along the incident axis [11, 12]. A term proportional to $1 + a\cos^2\theta^*$ that interpolates the background (dotted curve) is also included. A small nonuniformity of the signal acceptance in the c.m. angle is taken into account. The comparison to the data has $\chi^2/d.o.f. = 1.9/9$. Here the functions are normalized to the numbers of signal and background events obtained from the fit of the invariant mass dis-

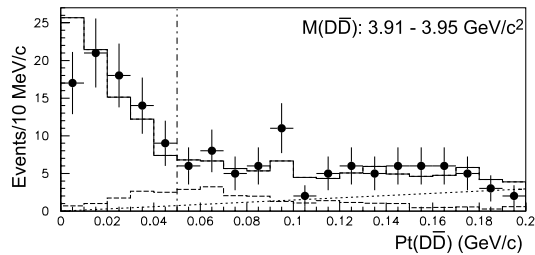


FIG. 3: Experimental $P_t(D\bar{D})$ distribution (points with error bars) for events in the $3.91 < M(D\bar{D}) < 3.95 \text{ GeV}/c^2$ region and the fit (histogram) based on the exclusive $\gamma\gamma \rightarrow D\bar{D}$ process MC plus a linear background (dotted line). The dot-dashed line shows the location of the P_t selection requirement. The dashed histogram shows the expected distribution of the $\gamma\gamma \rightarrow D\bar{D}^*$ process followed by $\bar{D}^* \rightarrow \bar{D}\pi$ with an arbitrary normalization.

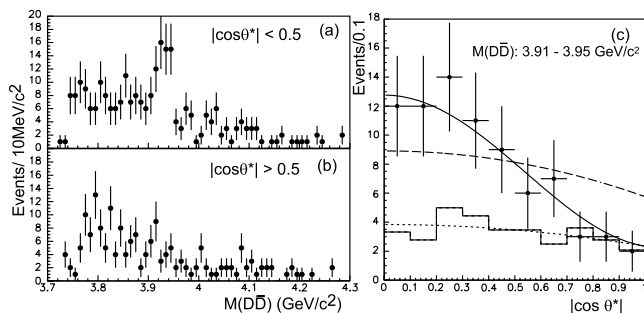


FIG. 4: $M(D\bar{D})$ distributions for (a) $|\cos\theta^*| < 0.5$ and (b) $|\cos\theta^*| > 0.5$. (c) The $|\cos\theta^*|$ distributions in the $3.91 < M(D\bar{D}) < 3.95 \text{ GeV}/c^2$ region (points with error bars) and background scaled from the $M(D\bar{D})$ sideband (solid histogram). The solid and dashed curves are expected distributions for the spin two (helicity two) and spin zero hypotheses, respectively, and contain the non-peak background also shown separately by the dotted curve.

tribution, 46 and 33 events, respectively. A comparison using a constant term to represent the signal from a spin-0 meson (dashed curve) gives a much poorer fit: $\chi^2/d.o.f. = 23.4/9$. The data significantly favor a spin two assignment over spin zero.

No charmonium state that decays into $D\bar{D}$ with a mass near $3.93 \text{ GeV}/c^2$ has been previously reported. This observation cannot be attributed to a new $J^{PC} = 1^{--}$ meson (ψ) produced by ISR processes, because there are no structures as large as the signal at this mass in the e^+e^- hadronic cross section.

Using the number of observed signal events, the branching fractions and efficiencies for the four decay channels, we determine the product of the two-photon decay width and $D\bar{D}$ branching fraction to be $\Gamma_{\gamma\gamma}(Z(3930))\mathcal{B}(Z(3930) \rightarrow D\bar{D}) = 0.18 \pm 0.05(stat) \pm 0.03(sys) \text{ keV}$, assuming production of a spin-2 meson. Here, we define $\mathcal{B}(Z(3930) \rightarrow D\bar{D}) = \mathcal{B}(Z(3930) \rightarrow D^0\bar{D}^0) + \mathcal{B}(Z(3930) \rightarrow D^+D^-)$ and as-

sume $\mathcal{B}(Z(3930) \rightarrow D^+D^-) = 0.89\mathcal{B}(Z(3930) \rightarrow D^0\bar{D}^0)$ according to isospin invariance and including the effect of the mass difference between D^0 and D^\pm mesons, where $Z(3930)$ is used as a tentative designation for the observed state.

We assign a 17% total systematic error to the measurement of the product of the two-photon decay width and the branching fraction, as shown in the above result. This is primarily due to uncertainties in the track reconstruction efficiency (7%), selection efficiency (8%), kaon identification (4%), choice of the fit function and background shape (5%), luminosity function (5%), and the D -meson branching fractions (9%), added in quadrature with other smaller factors.

The observed signals for the $D^0\bar{D}^0$ and D^+D^- modes are consistent with isospin invariance. The ratio of the branching fractions is measured to be $\mathcal{B}(Z(3930) \rightarrow D^+D^-)/\mathcal{B}(Z(3930) \rightarrow D^0\bar{D}^0) = 0.74 \pm 0.43(stat) \pm 0.16(sys)$. The results on mass, decay angular distributions and $\Gamma_{\gamma\gamma}\mathcal{B}(\rightarrow D\bar{D})$ are all consistent with expectations for the χ'_{c2} , the 2^3P_2 charmonium state [2, 3, 13].

In summary, we have observed an enhancement in $D\bar{D}$ invariant mass near $3.93 \text{ GeV}/c^2$ in $\gamma\gamma \rightarrow D\bar{D}$ events. The statistical significance of the signal is 5.3σ . The observed angular distribution is consistent with two-photon production of a tensor meson. Results for the mass, width, and the product of the two-photon decay width times the branching fraction to $D\bar{D}$ are: $M = 3929 \pm 5(stat) \pm 2(sys) \text{ MeV}/c^2$, $\Gamma = 29 \pm 10(stat) \pm 2(sys) \text{ MeV}$ and $\Gamma_{\gamma\gamma}\mathcal{B}(\rightarrow D\bar{D}) = 0.18 \pm 0.05(stat) \pm 0.03(sys) \text{ keV}$ (assuming $J = 2$), respectively. The measured properties are consistent with expectations for the previously unseen χ'_{c2} charmonium state.

We thank the KEKB group for excellent operation of the accelerator, the KEK cryogenics group for efficient solenoid operations, and the KEK computer group and the NII for valuable computing and Super-SINET network support. We acknowledge support from MEXT and JSPS (Japan); ARC and DEST (Australia); NSFC (contract No. 10175071, China); DST (India); the BK21 program of MOEHRD, and the CHEP SRC and BR (grant No. R01-2005-000-10089-0) programs of KOSEF (Korea); KBN (contract No. 2P03B 01324, Poland); MIST (Russia); MHEST (Slovenia); SNSF (Switzerland); NSC and MOE (Taiwan); and DOE (USA).

-
- [1] Belle Collaboration, S.-K. Choi *et al.*, Phys. Rev. Lett. **89**, 102001 (2002).
 - [2] S. Godfrey and N. Isgur, Phys. Rev. D **32**, 189 (1985).
 - [3] E. J. Eichten, K. Lane and C. Quigg, Phys. Rev. D **69**, 094019 (2004).
 - [4] Belle Collaboration, K. Abe *et al.*, hep-ex/0507019 (2005), submitted to Phys. Rev. Lett.

- [5] Belle Collaboration, S.-K. Choi *et al.*, Phys. Rev. Lett. **94**, 182002 (2005).
- [6] S. Kurokawa and E. Kikutani, Nucl. Instr. and Meth. A **499**, 1 (2003), and other papers included in this volume.
- [7] A. Abashian *et al.* (Belle Collab.), Nucl. Instr. and Meth. A **479**, 117 (2002).
- [8] S. Uehara, KEK Report 96-11 (1996).
- [9] H.-U. Bengtsson and T.Sjöstrand, Comp. Phys. Commun. **46**, 43 (1987); T.Sjöstrand, CERN preprint, TH-6488-92 (1992).
- [10] S.Eidelman *et al.* (PDG), Phys. Lett. B **592**, 1 (2004).
- [11] Belle Collaboration, K. Abe *et al.*, Phys. Lett. B **540**, 33 (2002).
- [12] M. Poppe, Int. J. Mod. Phys. A **1**, 545 (1986); H. Krasemann, J.A.M. Vermaseren, Nucl. Phys. B **184**, 269 (1981).
- [13] C.R. Münz, Nucl. Phys. A **609**, 364 (1996).